Catalyst-Free Thia-Michael Addition to alpha-Trifluoromethylacrylates for 3D Network Synthesis

Dimitri Berne, Sebastien Lemouzy, Pascale Guiffrey, Sylvain Caillol, Vincent Ladmiral, Eric Manoury, Rinaldo Poli, Eric Leclerc

Catalyst-Free Thia-Michael Addition to α-Trifluoromethylacrylates for 3D Network Synthesis

Dimitri Berne,[a] Sébastien Lemouzy,[a] Pascale Guiffrey,[a] Sylvain Caillol,[a] Vincent Ladmiral,[a] Eric Manoury,[b] Rinaldo Poli*[b,c] and Eric Leclerc*[a]

[a] D. Berne, Dr. S. Lemouzy, Dr. S. Caillol, Dr. V. Ladmiral, Dr. E. Leclerc
ICGM, Univ Montpellier, CNRS, ENSCM
34293 Montpellier Cedex 5 (France)
E-mail:
[b] Dr. E. Manoury, Prof. R. Poli
CNRS, LCC (Laboratoire de Chimie de Coordination), UPS, INPT
Université de Toulouse
205 route de Narbonne
31077 Toulouse, Cedex 4 (France)
E-mail:
[c] Prof. R. Poli
Institut Universitaire de France
1, rue Descartes
75231 Paris (France)

Supporting information for this article is given via a link at the end of the document.

Abstract: Thia-Michael additions (1,4-additions of a thiol to a Michael acceptor) are generally catalyzed by an external Brønsted or Lewis base. A spontaneous (uncatalyzed) Michael addition of thiols to α-trifluoromethyl acrylates is described in this article, as well as its application to the very efficient preparation of a thermoset. A thorough mechanistic investigation, based on an experimental kinetic study and on DFT calculations, is presented for the addition of arene- and alkanethiols to *tert*-butyl trifluoromethyl acrylate in polar aprotic solvents, unveiling a probable solvent-assisted proton transfer in the rate-determining step and a considerable lowering of the energy barrier induced by the CF_3 group.

Introduction

The thia-Michael addition is a nucleophilic conjugate (1,4-) addition of a sulfur nucleophile ("Michael donor") to the β-carbon atom of an electron poor alkene ("Michael acceptor") affording a thioether (thia-Michael adduct).[1] This reaction is generally base-catalyzed or nucleophile-initiated (Scheme 1). Weak Brønsted bases such as triethylamine induce a base-catalysis mechanism, whereas stronger Lewis bases such as phosphines lead to a nucleophile-initiated mechanism, the latter being the most widely used approach.[2,3] The first step of both mechanisms consists in the formation of a thiolate anion by deprotonation. This anion is of course obtained by acid-base reaction for the base-catalyzed mechanism. Regarding the nucleophilic initiation, an enolate is first formed by addition of the nucleophile onto the acceptor and then it reacts with the thiol to produce the initial thiolate anion.[4] After initiation, both mechanisms follow the same route. Hence, the generated thiolate adds to the electron-deficient β-carbon of the Michael acceptor to form the corresponding enolate adduct during the propagation step. Finally, a proton transfer occurs between a new thiol function and the enolate, which leads to the formation of the final product and of a new thiolate. The latter can then start a new thia-Michael addition cycle.[5] The thia-Michael addition was shown to be dependent on a few critical parameters such as solvent polarity,[6,7] base or initiator properties[8,9] and substrates design[10,11] (basicity of the Michael donor[9] and nature of the Michael acceptor[12]). Finally, mechanistic kinetic modelling have also been developed in order to predict the reactivity in thia-Michael additions according to the nature of the involved substrates and base/initiator.[13,14]

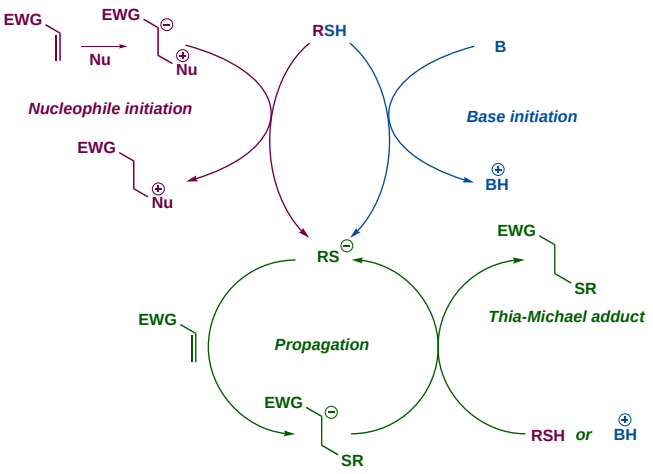

Scheme 1. Thia-Michael addition : nucleophile-initiated mechanism (top left) and base-catalyzed mechanism (top right).

The thia-Michael addition is one of the most common method in organic chemistry to create a C-S bonds. Thia-Michael adducts have been used to synthesize a large range of products including pharmaceutical agents, bioactive natural products, pesticides, food additives, surfactants and polymers.[8,14–21] In specific reference to polymer science, the thia-Michael addition has gained interest because of its rapidity and efficiency, mild reaction conditions and high tolerance towards many functional groups.[22] In addition, the thia-Michael addition is more selective

than the closely related radical-mediated thiol-ene reactions.[23] Indeed, secondary products are often obtained in the latter case through the homopolymerization of thiyl radicals.[24,25] Therefore, in opposition to the radical-initiated thiol-ene reaction, the polar thia-Michael addition can easily be performed in bulk or in dilute solutions.[23,26] Thia-Michael additions have been proved to be efficient "click" reactions in numerous applications[27,28] such as dendrimer synthesis,[29] surface functionalization,[30,31] bioconjugation[32–34] as well as in macromolecular engineering.[35–38] Moreover, the "click" reaction concept introduced by B. Sharpless *et al.*[39] is in line with many of the green chemistry principles,[40] making the thia-Michael addition a promising reaction for further development.

On the path of green chemistry development, reactions that can be carried out under solvent- and catalyst-free conditions have recently gained increasing attention. A few examples of catalyst-free thia-Michael reactions, mainly using peculiar nucleophiles such as thioureas or isothiocyanates to prepare thiazinone derivatives, have been reported.[27,41] The addition of thiols to very electron-deficient alkenes can also be performed under catalyst-free conditions. For instance, the addition of thioacetic acid on a variety of conjugated alkenes was demonstrated under solvent- and catalyst-free conditions, but requiring a large excess of thioacetic acid.[41] An efficient addition under catalyst-free conditions was also reported for nitroalkenes as Michael acceptors.[42] The effect of fluorinated groups on the reactivity of Michael acceptors was previously highlighted on model molecules by A. Fokin *et al*.[43] and J. Zhao *et al*.[44] The exceptional inductive effect of an α or β-trifluoromethyl substituent on the acceptor enabled the catalyst-free addition of aryl thiols. However, these two investigations were devoid of any kinetic and mechanistic studies, or of comparative studies with non-fluorinated substrates to assess the activating role of the CF_3 group. Therefore, in order to quantify this role, we have carried out a thorough study of the catalyst-free thia-Michael addition of two model thiols (thiophenol and *n*-octyl mercaptan) on *tert*-butyl α-trifluoromethylacrylate. A kinetic study coupled with DFT calculations allowed to improve the understanding of the catalyst-free thia-Michael addition mechanism. Finally, the high reactivity of α-trifluoromethyl acrylates in such a reaction was used to develop a new catalyst-free polymerization strategy leading to 3D networks.

Results and Discussion

Preliminary results.

The first goal was to qualitatively confirm the rate-enhancing effect of an α-CF_3 group on a Michael acceptor on the thiol addition using simple model molecules (Scheme 2). *Tert*-butyl α-trifluoromethyl acrylate (MAF-TBE) **2** was reacted with either thiophenol **1a** or *n*-octyl mercaptan **4** in THF at 50°C, without any external base. The addition products **3a** and **5** were quantitatively produced in less than 20 minutes or 1 h, respectively. A competition experiment has been performed to qualitatively compare the rates of addition of **1a** and **4**: the reaction involving equimolar amounts of **1a**, **4** and **2** in THF (1M concentration) at 50 °C yielded a 92:8 mixture of **3a** and **5** (only **3a** is produced at RT), confirming the greater reactivity of **3a** in this reaction.

In contrast to these results with MAF-TBE, no reaction occurred after 8 h with *tert*-butyl methacrylate (MA-TBE) **6**, under the same conditions, using either **1a** or **4** as the nucleophiles. Prolonged reaction times only resulted in degradation products, presumably through homopolymerization of **6**.

These striking results confirmed the occurrence of a fast thia-Michael addition to an α-trifluoromethyl acrylate without the need of an external base. In order to quantify the rate-enhancing effect of the α-CF_3 group, as well as to get some insight into the mechanism, we embarked on a mechanistic investigation combining experimental kinetics and DFT calculations.

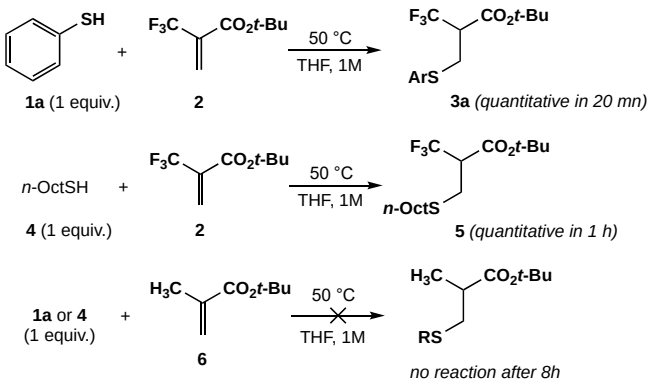

Scheme 2. Thia-Michael reactions on MAF-TBE **2** or MA-TBE **6**.

Experimental kinetic study.

The initial goal was to (i) quantitatively assess the effect of the CF_3 group on the Michael addition rate, (ii) establish the rate law and determine the rate constant and the activation parameters of a representative reaction and (iii) collect experimental data that would give some indications on the mechanistic pathway. Unfortunately, and as expected from our preliminary molecular study, a direct comparison of an uncatalyzed thio-Michael addition on a non-fluorinated and on a fluorinated acrylate was not possible, because the uncatalyzed addition of thiophenol **1a** to ethyl methacrylate or even ethyl acrylate was too sluggish, even at high temperatures, to allow any reliable kinetic measurement. We thus focused on the study of the addition of arenethiols onto MAF-TBE **2**.

The first task was to determine the experimental conditions (solvent, temperature) and to choose the analytical method that would be appropriate to perform a quantitative kinetic study. THF was used in the preliminary qualitative study but the reactions were too fast in this solvent (complete within 1 hour with PhSH at rt) to ensure an accurate measurement of the product concentrations. On the other hand, the reaction was found to proceed sluggishly in dichloromethane and not at all in benzene. Methyl *tert*-butyl ether (MTBE) adequately slowed down the reaction (completion reached after 4 h with PhSH) and was thus selected for the remainder of the study. These qualitative observations point to a significant polar character for the transition state, but also to an active role of the solvent basicity, because dichloromethane has a higher dielectric constant (ε = 8.93) than THF (7.4) and MTBE (4.50), but does not have basic properties. This suggests a possible involvement of proton transfer from the thiol in the rate-determining step. A monitoring of the reaction by ^{19}F NMR was carried out by diluting withdrawn aliquots in C_6D_6. The latter acted as an efficient quencher of the Michael addition. A control experiment showed that the relative quantities of the

reaction partners only marginally evolved after several hours following the dilution.

Under these conditions (Scheme 3), the reaction order in each reagent (**2** and **1a**) was first checked at 25°C. Using a large excess (10 equivalents, $[\mathbf{1a}]_0$ = 1 M) of **1a**, the plot of $\ln([\mathbf{2}]/[\mathbf{2}]_0$ *vs.* time (Figure 1a and data in Table S1) showed an unambiguous linear dependence (R^2 = 0.99) and yielded the value of the pseudo-first-order (observed) rate constant, $k_{obs} = (1.68\pm0.01)\cdot10^{-4}$ s^{-1}. Having proved that the reaction is first order in Michael acceptor, the reaction was also performed with 15 and 20 equivalents of the Michael donor **1a** (data in Tables S2 and S3) to check the k_{obs} dependence on $[\mathbf{1a}]_0$. The results (Figure S1, Table S4 and Figure 1b) indicate a more than acceptable linear (first-order) dependence. The statistical analysis of this fit yields $k = (1.93\pm0.15)\cdot10^{-4}$ $s^{-1}M^{-1}$ for the reaction rate constant at 25 °C. The slight k_{obs} deviation toward greater values relative to the best fit at higher $[\mathbf{1a}]_0$ is attributed to an increase of the medium polarity. A possible alternative interpretation of this deviation would involve the contribution of an additional second-order pathway, resulting from the participation of a second thiol molecule in a proton shuttle mechanism. Higher-order processes have previously been observed with implication of water or alcohols or amines as proton shuttle in proton transfer reactions such as transesterification and aminolysis.[45,46] However, this possibility seems discarded by the DFT calculations (*vide infra*).

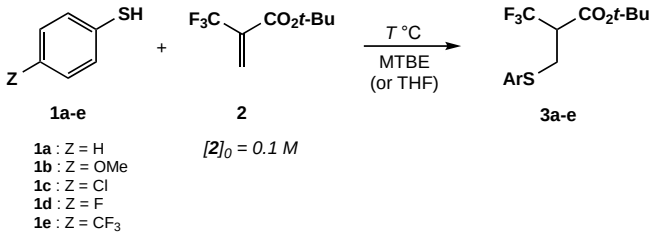

Scheme 3. General reaction for the kinetic study. $[\mathbf{2}]_0$ = 0.1 M. [**2**] was monitored by ^{19}F NMR after dilution of withdrawn reaction samples in C_6D_6.

At that point, we wished to probe the possible contribution of a more active proton shuttle molecule, namely water, on the rate of the thia-Michael addition. The reaction was thus monitored using (i) MTBE dried over 4Å molecular sieves (20 ppm of water according to Karl-Fischer (KF) titration), (ii) "wet" MTBE as received from the commercial supply (162 ppm of water according to KF titration) and (iii) MTBE with added water (5227 ppm according to KF titration). The determined pseudo-first order rate constants, k_{obs}, were respectively $(1.15\pm0.001)\cdot10^{-4}$ s^{-1}, $(1.31\pm0.02)\cdot10^{-4}$ s^{-1} and $(3.62\pm0.09)\cdot10^{-4}$ s^{-1} (see SI, Tables S5-S7 and Figures S2-S5 for details). The presence of water has thus a significant, but not particularly remarkable influence on the rate of the reaction, suggesting that water has indeed the power to open a competitive proton shuttle pathway. The observed effect, however, is too small to make a marked difference between the commercial solvent and the carefully dried one. However, in order to avoid any reproducibility issue, the following experiments were carried out using MTBE dried over molecular sieves.

In order to clarify the effect of the medium polarity and basicity, a Hammett study was undertaken to check the effect of the aryl thiol *para*-substituent on the kinetics, using a series of electron-donating and electron-withdrawing groups (**1b-e**). For each nucleophile, the rate data measured with $[\mathbf{1}]_0$ = 1 M (10 equivalents with respect to **2**) were again in agreement with a first order decay (see Tables S8-S11 and Figures S6-S9 for details), yielding the rate constants collected in Table 1. Quite remarkably, a strong electronic effect was observed, since *p*-$CF_3C_6H_4SH$ reacted 120 times faster than its methoxy-substituted analogue. A plot of $\log(k_X/k_H)$ as a function of σ^+_X gave a Hammett correlation with an excellent linear fit (R^2 = 0.995), see Figure 2. A rather high positive electronic effect (ρ = 2.38) was observed, which suggests a build-up of negative charge on the thiolate anion at the transition state level.

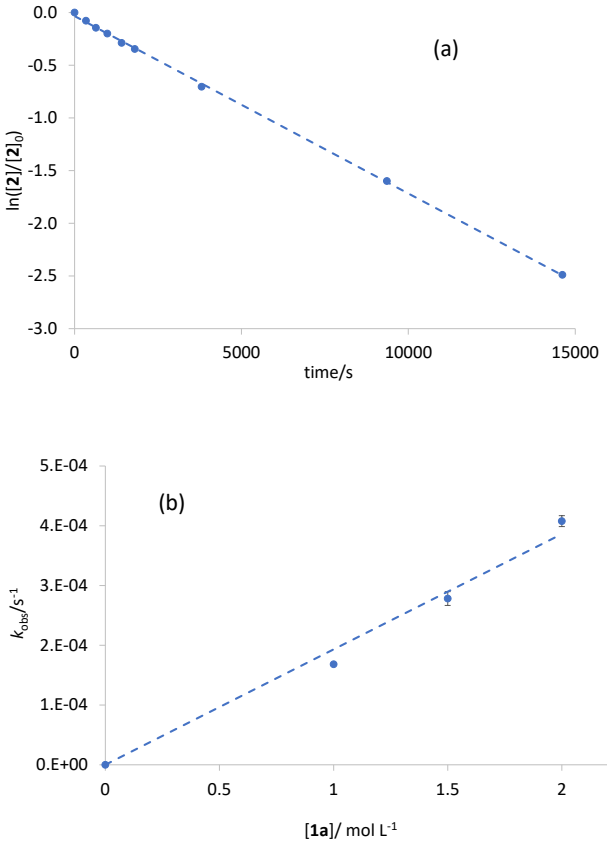

Figure 1. (a) Reaction monitoring for $[\mathbf{1a}]_0$ = 1M at 25 °C, and (b) plot of k_{obs} as a function of $[\mathbf{1a}]_0$ at 25 °C.

Table 1. Kinetic data and k_X/k_H for **1a-e** at 19.5±1 °C and for $[\mathbf{1}]_0$ = 1M

Thiol	X	σ^+(para)	$10^4 \cdot k$ (L mol^{-1} s^{-1})	log (k_X/k_H)
1a	H	/	1.15±0.01	/
1b	OMe	–0.268	0.24±0.01	–0.68±0.05
1c	F	0.062	1.28±0.05	0.05±0.04
1d	Cl	0.227	3.58±0.08	0.49±0.02
1e	CF_3	0.540	29.9±1.4	1.37±0.05

[a] $L.mol^{-1}.s^{-1}$

The activation parameters were determined on the basis of the rate constants determined at four different temperatures, using *p*-$MeOC_6H_4SH$ (**1b**) as the nucleophile. The lower reactivity of this thiol allows easier manipulations, more accurate

monitorings and the exploration of a wider temperature range. The reactions were performed at –1 °C, 8.6 °C, 18.6 °C and 29.3 °C (see SI, Tables S12-S16 and Figures S10-S13, for details). The Eyring-Polanyi plot, shown in Figure 3, exhibits a good linear fit (R^2 = 0.974) and yields $\Delta H^{\neq}$ = 11.0±1.3 kcal mol^{-1} and $\Delta S^{\neq}$ = –42.4±4.5 cal mol^{-1} K^{-1}. The negative activation entropy was of course expected from an associative process but its high value might suggest the involvement of additional solvent or nucleophile molecules in the transition state.

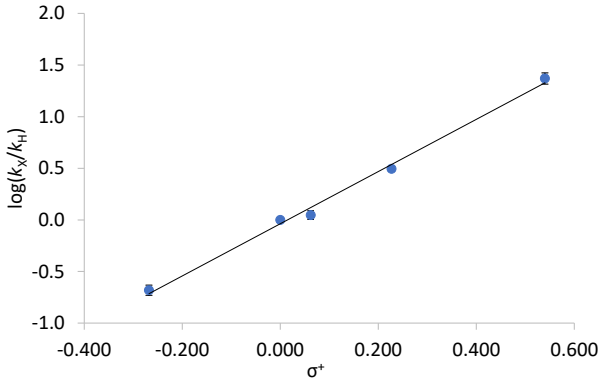

Figure 2. Hammett plot according to data of Table 1.

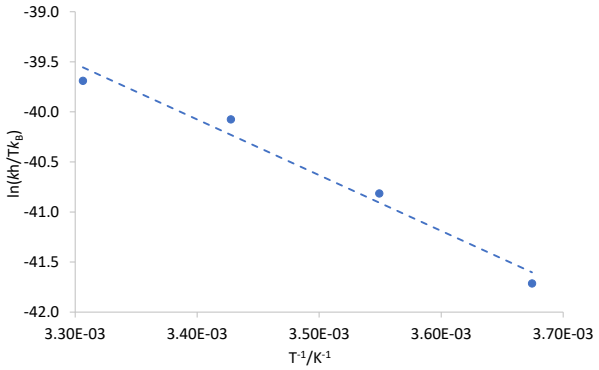

Figure 3. Eyring plot of the rate constants determined for the addition of **1b** to MAF-TBE at –1 °C, 8.6 °C, 18.6 °C and 29.3 °C in MTBE.

Finally, two additional experiments were carried out in order to further challenge the hypothesis that the thiol proton transfer is implicated in the rate-determining step. First, the rate of **1b** addition to **2** at -1.0 °C was also measured in THF (same conditions as the equivalent experiment in MTBE, Table S11 and Figure S13), giving rise to an approximately 9-fold acceleration (k_{MTBE} = 4.34±0.02·10^{-6} L mol^{-1} s^{-1} *vs* k_{THF} = (4.05±0.10)·10^{-5} L.mol^{-1}.s^{-1}, see Table S17 and Figure S14). Secondly, a kinetic experiment was also carried out for the addition of BnSH in MTBE at 29.3 °C, yielding a rate constant approximately four times smaller (k_{BnSH} = (9.0±0.3)·10^{-6} L mol^{-1} s^{-1}, see Table S18 and Figure S15) than for **1b** ($k_{\mathbf{1b}}$ = (3.65±0.09)·10^{-5} L.mol^{-1}.s^{-1}, Table S15 and Figure S13) . The facts that the reaction is faster in a more basic solvent such as THF and slower using a less acidic thiol are in perfect agreement with the dominating role of the thiol S-H heterolytic splitting in the transition state.

This experimental kinetic study therefore underlines the dramatic acceleration induced by the α-CF_3 group on the thia-Michael addition. Moreover, several experiments, including a Hammett plot, brought experimental support to the key role of the transfer of the thiol proton, with development of significant negative charge on the thiol S atom in the rate-determining step. The rate of this process is exalted by the solvent basicity (in the absence of any other external base).

DFT calculations.

This investigation was carried out in order to validate the mechanistic hypotheses formulated on the basis of the experimental kinetics studies, and to gather additional details on the nature of the rate-determining transition state. They used the same computational method that was previously used to explore the accelerating effect of the α-CF_3 group and of other F-substitution patterns on the transesterification reaction[47,48] (for the details, see the Experimental Section). The calculations were carried out on the addition of thiophenol and methyl mercaptan (as a smaller and electronically equivalent model of alkyl mercaptans) to CH_2=C(CX_3)COOMe (X = H, F), which were used as simpler models of MA-TBE and MAF-TBE, respectively. These substrates will henceforth be abbreviated as MMA (for X = H) and MMAF (for X = F). The replacement of the *tert*-butyl in the two esters and of the *n*-octyl group in the thiol with a methyl group speeds up the calculations while not significantly altering the electronic distribution in the reagents and products. A polarizable continuum correction was applied using the permittivity of the MTBE solvent (ε = 4.5) used for the experimental kinetics investigation. The Cartesian coordinates and energies of all optimized geometries (local minima and transition states) are collected in the Supporting Information. The thermodynamic gain of the addition reaction was calculated as slightly greater for the fluorinated system ($\Delta G_{MTBE,298K}$ = -8.8 and -8.0 kcal mol^{-1} for MeSH and PhSH, respectively) than for the non-fluorinated one (-4.6 and -5.9 kcal mol^{-1} for MeSH and PhSH, respectively).

A first mechanistic hypothesis consists of a thiol nucleophilic addition to the β-carbon to yield a zwitterionic intermediate $RSH^+CH_2C(CX_3)C(OMe)O^-$ (R = Me, Ph; X = H, F; see Scheme S1) that could then proceed to the product by proton transfer, either directly or upon proton shuttle assistance by a second thiol molecule. However, calculations on the Ph adducts could not locate any stable local minimum for the putative zwitterionic intermediate, all optimization attempts leading to H-bonded adducts, PhSH···CH_2=C(CX_3)COOMe (Figure S16). In these adducts, the thiol H atom interacts with the ester O atom of MMA (H···O = 2.337 Å) and with an F atom of MMAF (H···F = 2.324 Å). Next, a relaxed scan search was conducted on the C-S bond formation in the presence of a second PhSH molecule, which could assist the process as a proton shuttle by simultaneously removing the proton from the first PhSH molecule and delivering its own proton to the α-carbon atom (1,2 addition as shown in Scheme S1) or to the carbonyl O atom (1,4 addition). The starting point of the scan was the fully optimized PhSH···PhSH···CH_2=C(CX_3)COOMe adduct (Figure S17), where the second PhSH molecule acts as proton donor in H-bonding with the ester C=O group and as proton acceptor in H-bonding with the first PhSH molecule, which also shows an H···X contact with the methacrylate CX_3 group. In these adducts, there is no evident interaction between the attacking S atom and the acrylate β-C atom (separations > 3.5 Å). The scan for the X = H system, however, led to quite high energies at short C-S distances, with

the H atom of the second PhSH molecule remaining H-bonded to the ester carbonyl group but not showing any tendency to be transferred (see Figure S18). An alternative relaxed scan on a decreasing C···H distance equally revealed high energies and did not entail an approach of the S atom to the CH_2 group (Figure S19). Hence, a proton shuttle mechanism with thiol assistance and H transfer to the α-C atom seems excluded. A second hypothesis considered solvent assistance in the direct transfer of the thiol proton, without formation of a zwitterionic intermediate, from the thiol S atom to the methacrylate C atom (Scheme S2). Indeed, the presence of a Lewis basic ether solvent was experimentally shown to strongly promote the reaction (*vide supra*). The ether interaction with the transferring proton may assist the process *via* transition state stabilization, if the transferring proton markedly increases its protic character at the TS level. This mechanism was explored using Me_2O as a small model of the solvent molecule for the MeSH system. A TS geometry for this direct pathway could indeed be optimized for the MMAF system, but is located at $\Delta G^{\ddagger}_{MTBE,298K}$ = 31.7 kcal mol^{-1} relative to MMAF + MeSH···OMe_2 (Figure S5). Introducing a second ether molecule did not sufficiently improve the situation, as the barrier to transfer relative to MMAF + MeSH···$(OMe_2)_2$ was only slightly reduced to 29.2 kcal mol^{-1} (Figure S20). These barriers are too high to be compatible with the observed rate constants, excluding this mechanistic hypothesis.

Finally, the aptitude of the PhSH proton to establish an H-bond with the ester carbonyl O atom (Figure S17) suggested the possibility of a 1,4-addition, without a proton shuttle, leading to the ester enol form (Scheme S3), which could later rapidly tautomerize to the final ester structure. The exploration of this mechanism for both MeSH and PhSH additions to both MMA and MMAF gave Gibbs energy profiles that are more compatible with the experimentally measured rates. The profiles of the MeSH additions are shown in Figure 4 and those of the PhSH additions are presented in Figure 5. In particular, the MMAF system exhibits much lower barriers than the MMA system (by 6.3 kcal mol^{-1} for the MeSH addition and by 5.8 kcal mol^{-1} for the PhSH addition). The calculations also predict faster reactions for the additions of PhSH relative to MeSH (lower barrier by 1.7 kcal mol^{-1} for the addition to MMA and by 1.2 kcal mol^{-1} for the addition to MMAF). The rate ratios for the additions of the same thiol to the two systems at 25 °C are calculated as $4.1 \cdot 10^4$ for MeSH and $1.8 \cdot 10^4$ for PhSH in favour of the MMAF system. The predicted rate ratios for the additions of the two thiols to the same unsaturated ester at 25 °C are 17.6 for MMA and 7.6 for MMAF in favour of PhSH. The calculated barrier for the PhSH (**1a**) addition to MMAF (which can be decomposed into a 5.3 kcal mol^{-1} of enthalpic contribution and an activation entropy of -35.4 cal mol^{-1} K^{-1}) is in only qualitative agreement with the experimentally measured activation parameters for the addition of **1b** to MAF-TBE. The discrepancy can be attributed to several inadequacies, notably the neglect of the explicit interaction between the reactants and the solvent, the basicity of which was shown crucial in the experimental investigation. However, this calculated mechanism qualitatively reproduces the very negative activation entropy and the accelerating effects of the acrylate CH_3/CF_3 and thiol alkyl/aryl substitutions.

These calculated trends can be rationalized by electronic effects, as suggested by the Mulliken charges (see Figure S21). The substrate β-C atom is less negatively charged in MMAF (-0.087) than in MMA (-0.132), suggesting lower resistance by MMAF to receive the electron density of the S atom. This C atom becomes substantially more negative at the TS level and the charge further increases and becomes less substrate-dependent (in the -0.443 to -0.430 range) in the tautomeric intermediate. Of even greater interest is the evolution of the S atom charge: for the two MMAF reactions, the charge remains nearly neutral on going from free RSH to TS to product (-0.066/0.080/0.067 for MeSH; 0.035/0.009/0.096 for PhSH). On the other hand, the S atom becomes significantly more negative at the TS level for the two MMA reactions (-0.066/-0.138/0.050 for MeSH; 0.035/-0.132/0.077 for PhSH). This difference reflects an "earlier" proton transfer to the O atom (shorter H-O and longer S-H) and a "later" S binding to C (longer S-C) at the TS level for the MMA system. This reflects again the greater electrophilicity of the MMAF β-C atom. At the same time, the carbonyl O atom is more nucleophilic in MMA (-0.329) than in MMAF (-0.301). Hence, there is greater tendency for the MMA system to establish the O-H bond before the C-S bond, thus imparting a greater negative charge to the S atom in the TS, whereas the two transfers are more synchronous for the MMAF system, thus keeping the S atom more neutral.

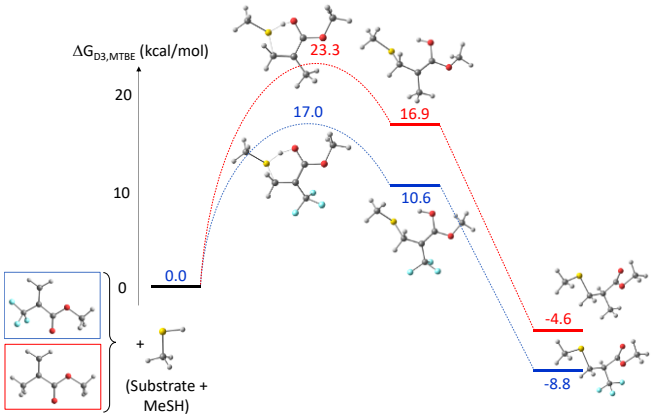

Figure 4. Gibbs energy profile for the 1,4 addition of MeSH to CH_2=C(CX_3)COOMe (X = H, F).

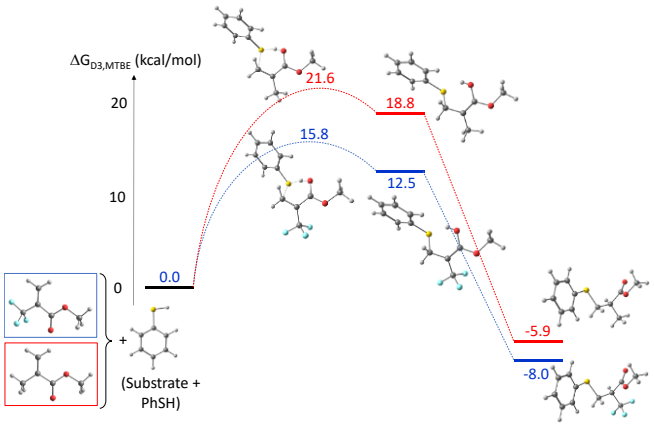

Figure 5. Gibbs energy profile for the 1,4 addition of PhSH to CH_2=C(CX_3)COOMe (X = H, F).

The faster PhSH addition relative to the MeSH addition does not result from the thiol nucleophilicity (C···S interaction), but rather from its acidity (H···O interaction). Indeed, MeSH carries a greater negative charge on the S atom. Inspection of the interatomic distances at the TS level (Figure S21) shows that, for the same ester substrate, the MeSH addition TS has a longer

H···O distance and a shorter C···S distance than the PhSH addition TS. This feature may also be the key to rationalize a violation to the Hammond principle: for both MMA and MMAF systems, the addition of thiophenol is more endergonic than that of methanethiol, but the energies of the TSs follow the opposite trend. This behavior is probably related to the greater cost of stretching the O-H bond and the lower gain related to the C-S bond formation.

A final DFT investigation involved the possible action of water as a proton shuttle for this reaction (Scheme S4). As shown above, a possible proton shuttle action by a second thiol molecule seems ruled out by the DFT investigation, but water has greater power than a thiol, both as a proton donor and as a proton acceptor in H-bonding, while the experimental work (*vide supra*) suggests that the reaction rate is sensitive to the water content in the solvent. This investigation was limited to the MeSH/MMAF system. The Gibbs energy barrier of this pathway (Figure 6), when considering the initial Gibbs energy cost of assembling the MeS···H_2O adduct from the separate molecules, is essentially identical to that of the direct 1,4 addition (Figure 4). The enol intermediate is also stabilized relative to that obtained by the direct 1,4 addition. This stabilization seems the consequence of the replacement of a weaker H-bond (S-H···OH_2) with a stronger one (O-H···OH_2), plus the establishment of an additional C-F···H-O interaction.

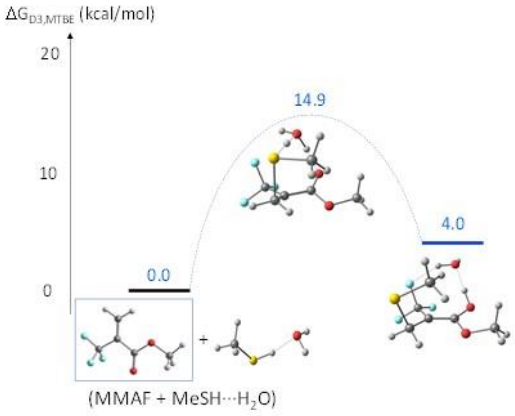

Figure 6. Gibbs energy profile for the 1,4 addition of MeSH to MMAF with proton shuttle assistance of a water molecule.

Calculations on the final step (ester enol tautomerization) were not carried out, as this process is not likely to be rate-determining.

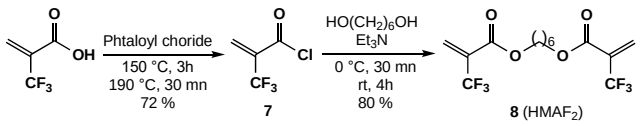

Scheme 4. Synthesis of the *bis*-trifluoromethacrylate ($HMAF_2$) monomer.

Thermosets preparation.

Following the kinetic and DFT studies, the activation effect of the α-CF_3 group was used to prepare crosslinked networks *via* thia-Michael additions. First, a difunctional trifluoromethacrylate **8** ($HMAF_2$) was synthesized by esterification of hexanediol with 2-(trifluoromethyl)acryloyl chloride **7** (MAF-Cl). MAF-Cl was isolated by distillation from the reaction of 2-(trifluoromethyl)acrylic acid with phtaloyl chloride (Scheme 4), and was characterized by ^{1}H, ^{19}F and ^{13}C NMR (Figure S29) and MS (Figure S32) analyses. The global reaction yield was 58 %.

Analogous fluorinated (**TF**) and non-fluorinated (**TNF**) thermosets were synthesized by thia-Michael polyaddition (Scheme 5). The synthesis of a non-fluorinated material based on a methacrylate motif was not possible because the thia-Michael addition did not proceed, even in presence of a catalyst. Instead, 1,6-hexanediol diacrylate (**10**, HA_2) was copolymerized with **9** (pentaerythritol *tetrakis*(3-mercaptopropionate), PETMP) in the presence of triethylamine as a catalyst at room temperature overnight to yield **TNF**. In contrast, **TF** was prepared from HDMAF and PETMP without any catalyst at 50 °C in 2 h and with a post-curing of one half-hour at 150 °C. Indeed, as demonstrated above, the thia-Michael addition onto trifluoromethyl acrylates proceeds readily under catalyst-free conditions. Rheological kinetic studies were carried out at 50 °C on the starting mixtures. For the HA_2 + PETMP (without NEt_3) solution, the viscosity profile did not evolve after 3 days at 50 °C, confirming that no reaction occurred without catalyst. For the $HMAF_2$ + PETMP solution, the gel point (crossing of G' and G'') was reached after 14 min (Figure 7). The remarkably strong activation effect induced by the trifluoromethyl group enabled a fast thia-Michael addition, which resulted in the rapid formation of the 3D network without any catalyst.

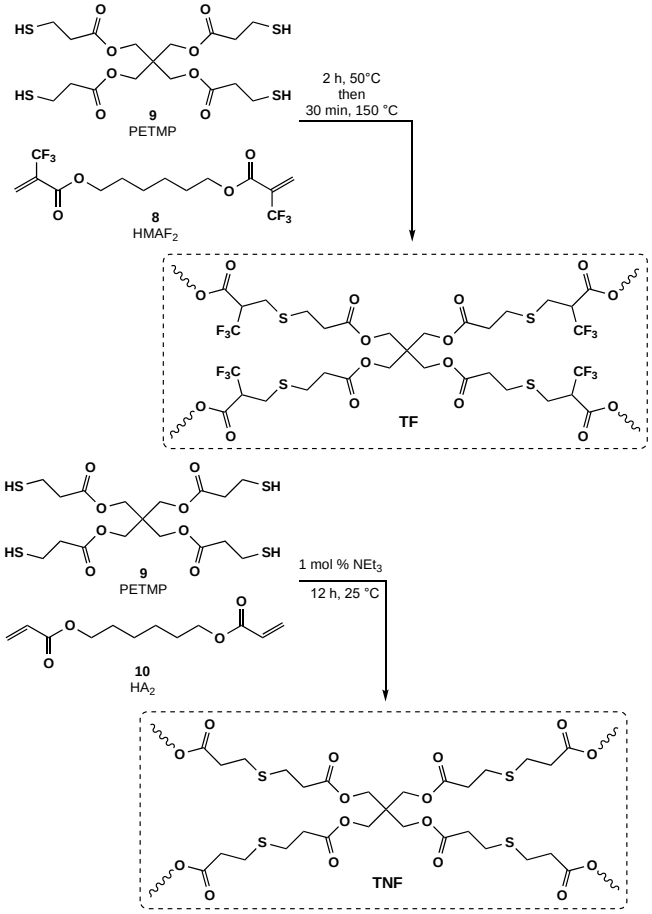

Scheme 5. Synthesis of **TF** from **9** and **8** and synthesis of **TNF** from **9** and **10**.

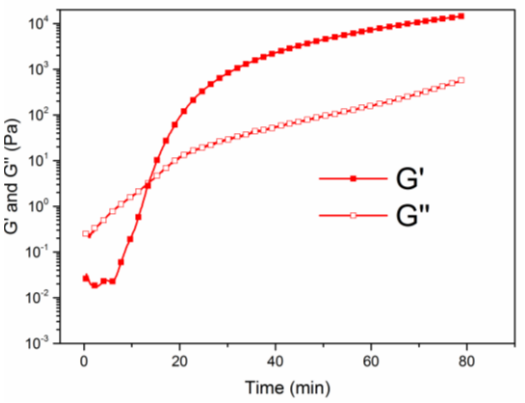

Figure 7. Evolution of G' (close square) and G'' (open square) with curing time for TF (red, full line) at a curing temperature of 50 °C

The chemical and physical properties of **TF** and **TNF** were evaluated by FTIR, TGA, DSC, DMA and water contact angle (Table 2). High insolubility ratios (>94%) were obtained for both materials, confirming the network formations. The swelling ratios of both materials were also very similar (≈ 170 %), as expected given their structural similarities. The characteristic C=C stretching bands of HDMAF (1636-1668 cm^{-1}) and HDA (1627-1650 cm^{-1}) and the S-H stretching band of PETMP (2454-2611 cm^{-1}) were no longer present in the FTIR spectra of **TF** (Figure 8) and **TNF** (Figure S22), further confirming the network formation for both materials. **TF** and **TNF** were shown by a TGA analysis to be thermally stable up to 330 °C (Figure S23) which allows using these materials in a broad temperature range.

Table 2. Chemical and mechanical properties of TF and TNF materials

	$T_d^{5\%}$ (°C)	T_g (°C)	T_α (°C)	E'_{glass} (GPa)	$E'_{rubbery}$ (MPa)	Swelling ratio[a] (%)	Insolubility ratio[a] (%)
TF	337	-0	21	2.8	10.8	174	95
TNF	362	- 21	- 2	2.4	10.1	171	94

[a] Tests performed in THF at room temperature for 24 h

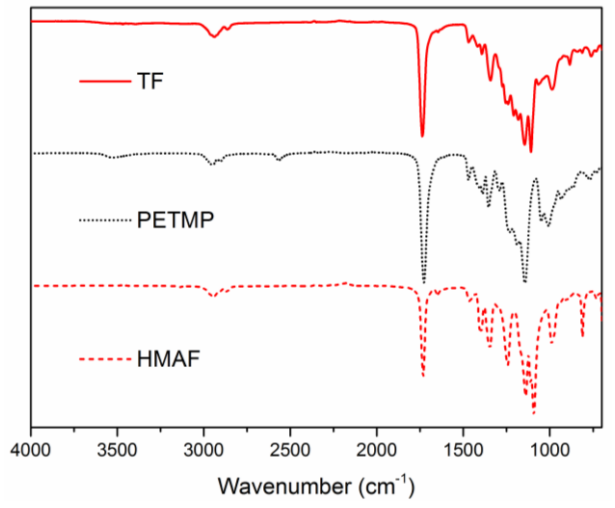

Figure 8. FTIR spectra of HDMAF (dashed red), PETMP (dotted black) and TF (full red).

The presence of CF_3 groups brings new properties to the material compared to its non-fluorinated equivalent. Indeed, higher T_g (Figure S24) and T_α were observed for **TF** ($\Delta T_g \approx \Delta T_\alpha \approx$ 20°C. This suggests that the presence of large CF_3 group in the networks reduces the chain mobility. The DMA analyses (Figure 9) highlighted that **TF** and **TNF** have similar moduli noth in the low and high-temperature regimes. These observations confirm that similar network structures were obtained for both materials. Finally, due to the hydrophobic properties of the trifluoromethyl groups, the water contact angle of **TF** is higher than that of **TNF** (Figure 10).

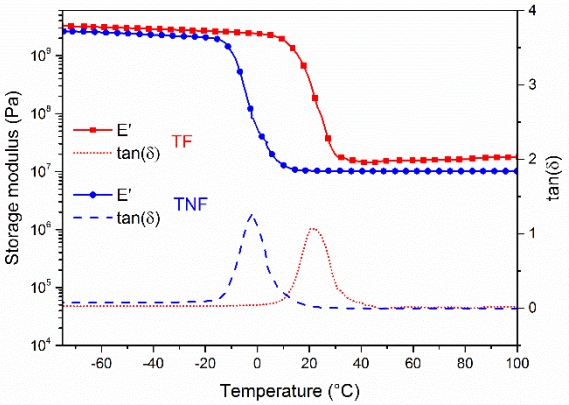

Figure 9. Storage modulus (E') and tan(δ) of **TF** (square and dotted red) and **TNF** (circle and dashed blue).

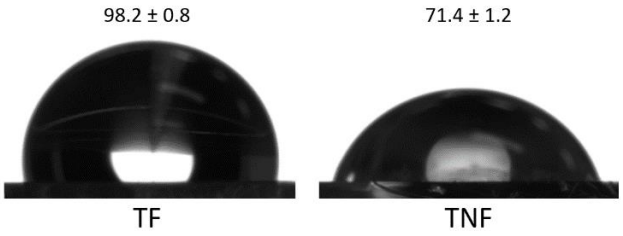

Figure 10. Water contact angle measurements of TF (left) and TNF (right)

Conclusion

The exceptional reactivity of α-(trifluoromethyl)acrylates (MAF-TBE in the kinetic investigations and $HMAF_2$ in the formation of the **TF** network) towards the thia-Michael addition was unambiguously demonstrated in the present study. Indeed, thiols undergo a rather uncommon catalyst-free addition to these Michael acceptors. The mechanism of this reaction is suggested by DFT calculations and experimentally supported by a kinetic study. Both approaches converge towards a mechanism featuring a 1,4-addition to yield an ester enol intermediate with transfer of the thiol proton in rate-determining step, as illustrated by the increased rates when using more acidic thiols or more basic solvents.

This exceptional reactivity was herein applied to the synthesis of a thermoset that was fastly prepared in the absence of any additive or catalyst, in contrast with its non-fluorinated counterpart.

This work opens the way to the future design of covalent adaptable networks or vitrimers based on this enhanced reactivity of the α-trifluoromethylacrylate moiety.

Experimental Section

Tert-butyl 2-(trifluoromethyl)acrylate (MAF-TBE, 98 %) was purchased from SynQuest Labs (Alachua, FL, USA). Benzyl mercaptan (99 %) and octanethiol (98.5 %) were purchased from Sigma Aldrich. Arylthiols (>98%) were all purchased from Fluorochem. 2-(Trifluoromethyl)acrylic acid (MAF) (>98 %) was purchased from SynQuest Labs (Alachua, FL, USA). 1,6-Hexanediol diacrylate with 100 ppm monomethyl ether hydroquinone as inhibitor (>90 %), pentaerythritol tetrakis(3-mercaptopropionate) (PETMP) (>95 %), phthaloyl chloride (> 90 %) and $CDCl_3$ were purchased from Sigma Aldrich (Darmstadt Germany). All the chemicals were used as received.

Synthesis of thia-Michael adducts 3a, 5 and 7

In a flame-dried round-bottom flask was charged MAF-TBE **2** (2 mmol), dissolved in THF (2 ml). Then, the appropriate thiol was added dropwise at room temperature, and the reaction was stirred for 3 h. The solvent was removed under vacuum, and the crude product was purified by column chromatography on silica gel (100% pentane → 95/5 pentane / AcOEt) the yield the pure products.

tert-butyl 3,3,3-trifluoro-2-((phenylthio)methyl) propanoate ***3a*** was obtained according to this procedure using thiophenol **1a** as the nucleophile, in the form of a colorless liquid (441 mg, 72%). **^{1}H-NMR** (300 MHz, DMSO) δ = 7.47 – 7.35 (m, 4H), 7.34 – 7.26 (m, 1H), 3.56 – 3.40 (m, 2H), 3.32 – 3.23 (m, 1H), 1.42 (s, 9H). **^{19}F-NMR** (282 MHz, DMSO) δ = -66. 8 (d, $^3J_{H\text{-}F}$ = 8.5 Hz). **^{13}C-NMR** (101 MHz, DMSO) δ = 164.9 (d, $^3J_{C\text{-}F}$ = 3.1 Hz), 134.3, 130.2, 129.8, 128.6-120.5 (q, $^1J_{C\text{-}F}$ = 281.4 Hz), 127.5, 83.4, 50.7 (q, $^2J_{C\text{-}F}$ = 26.0 Hz), 40.29 (q, $^1J_{C\text{-}F}$ = 42.0 Hz), 29.8 – 29.7 (q, $^3J_{C\text{-}F}$ = 4.6 Hz), 27.8. **HRMS** (ESI+): calc. m/z for $[M\text{-}H]^+$: 307.0974, measured: 307.0975.

tert-butyl 3,3,3-trifluoro-2-((octylthio)methyl) propanoate ***5*** was obtained according to this procedure using octanethiol **4** as the nucleophile, in the form of a colorless liquid (437 mg, 64%). **^{1}H-NMR** (400 MHz, $CDCl_3$) δ = 3.29-3.19 (m, 1H), 3.01 – 3.84 (m, 2H), 2.59-2.55 (t, 2H), 1.63-1.53 (m, 2H), 1.53 (s, 9H), 1.42-1.30 (m, 10 H), 0.93-0.89 (t, 2H). **^{19}F-NMR** (377 MHz, $CDCl_3$) δ = -68.31 (d, $^3J_{H\text{-}F}$ = 8.2 Hz). **^{13}C-NMR** (101 MHz, $CDCl_3$) δ = 165.3 (d, $^3J_{C\text{-}F}$ = 3.1 Hz), 127.5-119.91 (q, $^1J_{C\text{-}F}$ =281.3), 83.2, 52.6-51.8 (q, $^2J_{C\text{-}F}$ = 26.5 Hz), 32.6, 31.8, 29.4, 29.2, 29.1, 28.8, 27.9, 27.8 (q, $^3J_{C\text{-}F}$ = 2.5 Hz), 22.7, 14.1. **HRMS** (ESI+): calc. m/z for $[M\text{-}H]^+$: 343.1913, measured: 343.1917.

tert-butyl 3,3,3-trifluoro-2-((benzylthio)methyl) propanoate ***7*** was obtained according to this procedure using benzyl mercaptan as the nucleophile, in the form of a colorless liquid (441 mg, 72%). **^{1}H-NMR** (300 MHz, DMSO) δ = 7.38 – 7.30 (m, 4H), 7.26 (m, 1H), 3.84 (s, 2H), 3.70 – 3.53 (m, 1H), 2.76 (qd, $J_{H\text{-}F}$ = 13.7, $J_{H\text{-}H}$ = 7.4 Hz, 2H), 1.44 (s, 9H).**^{19}F-NMR** (282 MHz, DMSO) δ = -66.9 (d, $^3J_{H\text{-}F}$ = 8.8 Hz). **^{13}C-NMR** (101 MHz, DMSO) δ = 165.3 (q, $^3J_{C\text{-}F}$ = 5.6 Hz), 138.4, 129.4, 128.9, 127.5, 126.2, (q, $^1J_{C\text{-}F}$ =282.8 Hz) 83.1, 50.6 (q, $^2J_{C\text{-}F}$ = 25.7 Hz), 35.4, 27.9, 26.77 (q, $^3J_{C\text{-}F}$ = 4.7 Hz). **HRMS** (ESI+): calc. m/z for $[M\text{-}Na]^+$: 343.0950, measured: 343.0950.

Procedure for the competition experiments

In a flame-dried round-bottom flask was charged MAF-TBE **2** (1 mmol, 1 eq.) dissolved in THF (1 mL). Then, octanethiol **4** (1 mmol, 1 eq.) and thiophenol **1a** (1 mmol, 1 eq.) were added at room temperature or at 50 °C. The conversion and the **3a**/**5** ratio were measured and monitored by ^{19}F-NMR.

Procedure for the kinetic experiments

A flame-dried 10 ml scintillation vial was charged with MAF-TBE (0.25 mmol), dissolved in MTBE (pre-dried over 4A molecular sieves; the MTBE volume was adjusted so that the total reaction volume was 2.5 mL). After stirring at the appropriate temperature for 5 minutes, the corresponding thiol (2.5 mmol, 10 equiv) was rapidly added and the MZF-TBE conversion values were determined by integration of the ^{19}F NMR of withdrawn aliquots. The solutions used for the NMR measurements were obtained by diluting 100 µl of the reaction mixture in approximately 300 µl of C_6D_6.

Synthesis of 7 (MAF-Cl)

2-Trifluoromethylacryloyl chloride (MAF-Cl) was synthesized by the reaction of 2-trifluoromethylacrylic acid (MAF) (29.1 g, 208 mmol) with phthaloyl dichloride (63.2 g, 311.3 mmol) at 150 °C for 2 h and then 190 °C for 30 min in absence of solvent. The product was collected by distillation during reaction. Yield: 72 %, 23.8 g; bp = 82 °C.

Synthesis of 8 ($HMAF_2$)

NEt_3 (7.32 g, 72.4 mmol) was added dropwise to a dichloromethane solution of 1,6-hexanediol (2.85 g, 24.1 mmol) and MAF-Cl (9.56 g, 60.3 mmol) at 0 °C, followed by stirring at room temperature for 4 h. The reaction mixture was washed with 0.5 N hydrochloric acid, saturated aqueous sodium hydrogen carbonate and brine, treated with $MgSO_4$, filtered and dried under reduced pressure to afford the pure di-(trifluoromethacrylate) ($HMAF_2$). Yield: 80 %, 7.0 g. **^{1}H-NMR** (400 MHz, $CDCl_3$) δ = 6.75 (q, $^3J_{H\text{-}H}$ =1.7 Hz, 2H), 6.45 (q, $^3J_{H\text{-}H}$ =1.3 Hz, 2H), 4.29 (t,$^3J_{H\text{-}H}$ = 6.5 Hz, 4H), 1.72-1.79 (m, 4H), 1.45-1.49 (m, 4H). **^{19}F-NMR** (377 MHz, $CDCl_3$) δ = 65.7. **^{13}C-NMR** (101 MHz, $CDCl_3$) δ = 161.2, 132.7 (q, $^3J_{C\text{-}F}$ = 5.1 Hz), 130.9-131.9 (q, $^2J_{C\text{-}F}$ = 31.7 Hz), 117.3-125.4 (q, $^1J_{C\text{-}F}$ = 272.6 Hz), 65.6, 28.2, 25.3. **HRMS** (ESI+): calc. m/z for $[M\text{-}H]^+$: 363.1026, measured: 363.1024.

Synthesis of fluorinated thermoset (TF)

Fluorinated thermoset (TF) was synthesized from PETMP (x g, x eq.) and $HMAF_2$ (x g, x eq.). The reactive mixture was initially mixed 2 min using a SpeedMixer. Then TF was left 2 h at 50 °C, before to be post-cured at 150 °C for 30 min.

Synthesis of non-fluorinated thermoset (TNF)

Non-fluorinated thermoset (TNF) was synthesized from PETMP (x g, x eq.) and HA_2 (x g, x eq.) in presence of 1 mol % of triethylamine (NEt_3). The reactive mixture was initially mixed 2 min using a SpeedMixer. Then TNF was left at room temperature overnight.

High-resolution mass spectrometry (HRMS)

The high-resolution mass spectra were recorded on a Bruker Daltonics micrOTOF-Q with an ESI source and a positive ion polarity.

Fourier-transform infrared spectroscopy (FTIR)

Fourier-transform infrared spectra were recorded in the ATR mode on a Nicolet 210 FTIR instrument. The characteristic IR absorptions mentioned in the text are reported in cm^{-1}.

Differential scanning calorimetry (DSC)

The DSC analyses were carried out using a NETZSCH DSC200F3 calorimeter, which was calibrated using indium, *n*-octadecane and *n*-octane standards. Nitrogen was used as purge gas. Approximately 10 mg of sample were placed in a perforated aluminium pan and measured

between -150 °C and 200 °C at 20 K min^{-1}. The T_g values were obtained from the second heating ramp to erase the thermal history of the polymer.

Thermogravimetric analyses (TGA)

The TGA were carried out using a TG 209F1 apparatus (Netzsch). Approximately 10 mg of sample were placed in an aluminium oxide crucible and heated from room temperature to 500 °C at a heating rate of 20 °C min^{-1} under a nitrogen atmosphere (40 mL/min).

Swelling index (SI)

Three samples of the same material, each one weighing around 40 mg, were separately immersed in 10 mL of THF for 24 h. The SI was calculated using Equation 1, where m_2 is the mass of the swollen material and m_1 is the initial mass. The reported swelling indexes are averages of those measured for the independent samples.

$$SI = (m_2 - m_1)/m_1 \times 100$$

Equation 1. Swelling index

Gel Content (GC)

After the SI measurements, the same three samples were dried in a ventilated oven at 80 °C for 24 h. The GC was calculated using Equation 2, where m_3 is the mass of the dried material and m_1 is the initial mass. The reported gel contents are the average values of the three samples.

$$GC = m_3/m_1 \times 100$$

Equation 2. Gel content

Dunamic mechanical analyses (DMA)

The DMA were carried out with a Metravib DMA 25 using Dynatest 6.8 software. The samples were tested in uniaxial tension mode while heating at a rate of 3 °C min^{-1} at a frequency of 1 Hz and a fixed strain of 10^{-5} m.

Rheology

Rheology experiments were performed on a Thermo Fisher HAAKE MARS 60 rheometer. The gelation times were measured with a plate-plate geometry with a diameter of 25 mm. The gelation times were analyzed by observing the crossover of the storage modulus (G') and loss modulus (G") during an oscillatory experiment at 1 Hz, 50 °C and 1% of deformation, according to the previously determined linear domain.

Water contact angle (WCA)

The WCA measurements were carried out on a Data Physics OCA contact angle system. The water sessile drop method was used for the static contact angle (CA) measurements at ambient temperature. The probe liquid was water and the average CA value was determined on five different drops of ca. 10.0 µL deposited on the same sample.

Computational details

The computational work was carried out using the Gaussian09 suite of programs.[49] The geometry optimizations were performed without any symmetry constraint using the BP86 functional and the 6-311G(d,p) basis functions for all atoms. The effects of dispersion forces (Grimme's D3 empirical method[50]) and solvation (SMD,[51] ε = 4.5) were included during the optimization. The ZPVE, PV, and TS corrections at 298 K were obtained with Gaussian09 from the solution of the nuclear equation using the standard ideal gas and harmonic approximations at T = 298.15 K, which also verified the nature of all optimized geometries as local minima or first-order saddle points. A correction of 1.95 kcal/mol was applied to all G values to change the standard state from the gas phase (1 atm) to solution (1 M).[52]

Acknowledgements

The French National Research Agency (ANR) is gratefully acknowledged for funding this research (AFCAN program, ANR-19-CE06-0014). RP is grateful to the CALMIP mesocenter of the University of Toulouse for the allocation of computational resources.

Keywords: fluorine effect • Michael addition • DFT calculations • kinetics • thermosets

(1) Mather, B. D.; Viswanathan, K.; Miller, K. M.; Long, T. E. Michael Addition Reactions in Macromolecular Design for Emerging Technologies. *Prog. Polym. Sci.* **2006**, *31* (5), 487–531. https://doi.org/10.1016/j.progpolymsci.2006.03.001.

(2) Guang-Zhao Li; K. Randev, R.; H. Soeriyadi, A.; Gregory Rees; Cyrille Boyer; Zhen Tong; P. Davis, T.; Remzi Becer, C.; M. Haddleton, D. Investigation into Thiol-(Meth)Acrylate Michael Addition Reactions Using Amine and Phosphine Catalysts. *Polym. Chem.* **2010**, *1* (8), 1196–1204. https://doi.org/10.1039/C0PY00100G.

(3) Nair, D. P.; Podgórski, M.; Chatani, S.; Gong, T.; Xi, W.; Fenoli, C. R.; Bowman, C. N. The Thiol-Michael Addition Click Reaction: A Powerful and Widely Used Tool in Materials Chemistry. *Chemistry of Materials*. American Chemical Society January 14, 2014, pp 724–744. https://doi.org/10.1021/cm402180t.

(4) Chan, J. W.; Hoyle, C. E.; Lowe, A. B.; Bowman, M. Nucleophile-Initiated Thiol-Michael Reactions: Effect of Organocatalyst, Thiol, and Ene. *Macromolecules* **2010**, *43* (15), 6381–6388. https://doi.org/10.1021/ma101069c.

(5) Long, K. F.; Wang, H.; Dimos, T. T.; Bowman, C. N. Effects of Thiol Substitution on the Kinetics and Efficiency of Thiol-Michael Reactions and Polymerizations. *Macromolecules* **2021**, *54* (7), 3093–3100. https://doi.org/10.1021/acs.macromol.0c02677.

(6) Nguyen, L.-T. T.; Gokmen, M. T.; Prez, F. E. Du. Kinetic Comparison of 13 Homogeneous Thiol–X Reactions. *Polym. Chem.* **2013**, *4* (22), 5527–5536. https://doi.org/10.1039/C3PY00743J.

(7) Lowe, A. B. Thiol-Ene "Click" Reactions and Recent Applications in Polymer and Materials Synthesis. *Polym. Chem.* **2010**, *1* (1), 17–36. https://doi.org/10.1039/B9PY00216B.

(8) Xi, W.; Peng, H.; Aguirre-Soto, A.; Kloxin, C. J.; Stansbury, J. W.; Bowman, C. N. Spatial and Temporal Control of Thiol-Michael Addition via Photocaged Superbase in Photopatterning and Two-Stage Polymer Networks Formation. *Macromolecules* **2014**, *47* (18), 6159–6165. https://doi.org/10.1021/ma501366f.

(9) Northrop, B. H.; Frayne, S. H.; Choudhary, U. Thiol–Maleimide "Click" Chemistry: Evaluating the Influence of Solvent, Initiator, and Thiol on the Reaction Mechanism, Kinetics, and Selectivity. *Polym. Chem.* **2015**, *6* (18), 3415–3430. https://doi.org/10.1039/C5PY00168D.

(10) Huang, S.; Kim, K.; Musgrave, G. M.; Sharp, M.; Sinha, J.;

Stansbury, J. W.; Musgrave, C. B.; Bowman, C. N. Determining Michael Acceptor Reactivity from Kinetic, Mechanistic, and Computational Analysis for the Base-Catalyzed Thiol-Michael Reaction. *Polym. Chem.* **2021**, *12* (25), 3619–3628. https://doi.org/10.1039/D1PY00363A.

(11) Long, K. F.; Bongiardina, N. J.; Mayordomo, P.; Olin, M. J.; Ortega, A. D.; Bowman, C. N. Effects of 1°, 2°, and 3° Thiols on Thiol–Ene Reactions: Polymerization Kinetics and Mechanical Behavior. *Macromolecules* **2020**, *53* (14), 5805–5815. https://doi.org/10.1021/acs.macromol.0c00369.

(12) Nguyen, L. T. T.; Gokmen, M. T.; Du Prez, F. E. Kinetic Comparison of 13 Homogeneous Thiol–X Reactions. *Polym. Chem.* **2013**, *4* (22), 5527–5536. https://doi.org/10.1039/C3PY00743J.

(13) Claudino, M.; Zhang, X.; Alim, M. D.; Podgórski, M.; Bowman, C. N. Mechanistic Kinetic Modeling of Thiol-Michael Addition Photopolymerizations via Photocaged "Superbase" Generators: An Analytical Approach. *Macromolecules* **2016**, *49* (21), 8061–8074. https://doi.org/10.1021/ACS.MACROMOL.6B01605.

(14) Huang, S.; Sinha, J.; Podgórski, M.; Zhang, X.; Claudino, M.; Bowman, C. N. Mechanistic Modeling of the Thiol–Michael Addition Polymerization Kinetics: Structural Effects of the Thiol and Vinyl Monomers. *Macromolecules* **2018**, *51* (15), 5979–5988. https://doi.org/10.1021/acs.macromol.8b01264.

(15) Liu, G.; Link, J. T.; Pei, Z.; Reilly, E. B.; Leitza, S.; Nguyen, B.; Marsh, K. C.; Okasinski, G. F.; Von Geldern, T. W.; Ormes, M.; Fowler, K.; Gallatin, M. Discovery of Novel P-Arylthio Cinnamides as Antagonists of Leukocyte Function-Associated Antigen-1/Intracellular Adhesion Molecule-1 Interaction. 1. Identification of an Additional Binding Pocket Based on an Anilino Diaryl Sulfide Lead. *J. Med. Chem.* **2000**, *43* (21), 4025–4040. https://doi.org/10.1021/JM0002782.

(16) Yang, D. J.; Chen, B. Simultaneous Determination of Nonnutritive Sweeteners in Foods by HPLC/ESI-MS. *J. Agric. Food Chem.* **2009**, *57* (8), 3022–3027. https://doi.org/10.1021/JF803988U.

(17) Matsuno, R.; Takami, K.; Ishihara, K. Simple Synthesis of a Library of Zwitterionic Surfactants via Michael-Type Addition of Methacrylate and Alkane Thiol Compounds. *Langmuir* **2010**, *26* (16), 13028–13032. https://doi.org/10.1021/la1015466.

(18) Alswieleh, A. M.; Cheng, N.; Canton, I.; Ustbas, B.; Xue, X.; Ladmiral, V.; Xia, S.; Ducker, R. E.; El Zubir, O.; Cartron, M. L.; Hunter, C. N.; Leggett, G. J.; Armes, S. P. Zwitterionic Poly(Amino Acid Methacrylate) Brushes. *J. Am. Chem. Soc.* **2014**, *136* (26), 9404–9413. https://doi.org/10.1021/ja503400r.

(19) Dunbar, K. L.; Scharf, D. H.; Litomska, A.; Hertweck, C. Enzymatic Carbon–Sulfur Bond Formation in Natural Product Biosynthesis. *Chem. Rev.* **2017**, *117* (8), 5521–5577. https://doi.org/10.1021/acs.chemrev.6b00697.

(20) Jiang, K.; Wang, J.; Zuo, C.; Li, S.; Li, S.; He, D.; Peng, H.; Xie, X.; Poli, R.; Xue, Z. Facile Fabrication of Polymer Electrolytes via Lithium Salt-Accelerated Thiol-Michael Addition for Lithium-Ion Batteries. *Macromolecules* **2020**, *53* (17), 7450–7459. https://doi.org/10.1021/acs.macromol.0c01302.

(21) Zhang, X.; Xi, W.; Gao, G.; Wang, X.; Stansbury, J. W.; Bowman, C. N. O-Nitrobenzyl-Based Photobase Generators: Efficient Photoinitiators for Visible-Light Induced Thiol-Michael Addition Photopolymerization. *ACS Macro Lett.* **2018**, *7* (7), 852–857. https://doi.org/10.1021/acsmacrolett.8b00435.

(22) Hoyle, C. E.; Lowe, A. B.; Bowman, C. N. Thiol-Click Chemistry: A Multifaceted Toolbox for Small Molecule and Polymer Synthesis. *Chem. Soc. Rev.* **2010**, *39* (4), 1355–1387. https://doi.org/10.1039/B901979K.

(23) Kade, M. J.; Burke, D. J.; Hawker, C. J. The Power of Thiol-Ene Chemistry. *J. Polym. Sci. Part A Polym. Chem.* **2010**, *48* (4), 743–750. https://doi.org/10.1002/POLA.23824.

(24) Koo, S. P. S.; Stamenović, M. M.; Prasath, R. A.; Inglis, A. J.; Prez, F. E. Du; Barner-Kowollik, C.; Camp, W. Van; Junker, T. Limitations of Radical Thiol-Ene Reactions for Polymer–Polymer Conjugation. *J. Polym. Sci. Part A Polym. Chem.* **2010**, *48* (8), 1699–1713. https://doi.org/10.1002/POLA.23933.

(25) Derboven, P.; D'hooge, D. R.; Stamenovic, M. M.; Espeel, P.; Marin, G. B.; Prez, F. E. Du; Reyniers, M.-F. Kinetic Modeling of Radical Thiol–Ene Chemistry for Macromolecular Design: Importance of Side Reactions and Diffusional Limitations. *Macromolecules* **2013**, *46* (5), 1732–1742. https://doi.org/10.1021/MA302619K.

(26) Hoyle, C. E.; Bowman, C. N.; Bowman, C. N.; Hoyle, C. E. Thiol–Ene Click Chemistry. *Angew. Chemie Int. Ed.* **2010**, *49* (9), 1540–1573. https://doi.org/10.1002/ANIE.200903924.

(27) Wadhwa, P.; Kharbanda, A.; Sharma, A. Thia-Michael Addition: An Emerging Strategy in Organic Synthesis. *Asian J. Org. Chem.* **2018**, *7* (4), 634–661. https://doi.org/10.1002/AJOC.201700609.

(28) Nair, D. P.; Podgórski, M.; Chatani, S.; Gong, T.; Xi, W.; Fenoli, C. R.; Bowman, C. N. The Thiol-Michael Addition Click Reaction: A Powerful and Widely Used Tool in Materials Chemistry. *Chem. Mater.* **2014**, *26* (1), 724–744. https://doi.org/10.1021/cm402180t.

(29) Chatani, S.; Podgórski, M.; Wang, C.; Bowman, C. N. Facile and Efficient Synthesis of Dendrimers and One-Pot Preparation of Dendritic–Linear Polymer Conjugates via a Single Chemistry: Utilization of Kinetically Selective Thiol–Michael Addition Reactions. *Macromolecules* **2014**, *47* (15), 4894–4900. https://doi.org/10.1021/ma501418r.

(30) Tedja, R.; Soeriyadi, A. H.; Whittaker, M. R.; Lim, M.; Marquis, C.; Boyer, C.; Davis, T. P.; Amal, R. Effect of TiO2 Nanoparticle Surface Functionalization on Protein Adsorption, Cellular Uptake and Cytotoxicity: The Attachment of PEG Comb Polymers Using Catalytic Chain Transfer and Thiol–Ene Chemistry. *Polym. Chem.* **2012**, *3* (10), 2743–2751. https://doi.org/10.1039/C2PY20450A.

(31) Khire, V. S.; Lee, T. Y.; Bowman, C. N. Surface Modification Using Thiol−Acrylate Conjugate Addition Reactions. *Macromolecules* **2007**, *40* (16), 5669–5677. https://doi.org/10.1021/MA070146J.

(32) Ferruti, P.; Bianchi, S.; Ranucci, E.; Chiellini, F.; Caruso, V. Novel Poly(Amido-Amine)-Based Hydrogels as Scaffolds for Tissue Engineering. *Macromol. Biosci.* **2005**, *5* (7), 613–622. https://doi.org/10.1002/MABI.200500020.

(33) Richardson, S. C. W.; Pattrick, N. G.; Stella Man, Y. K.; Ferruti, P.; Duncan, R. Poly(Amidoamine)s as Potential Nonviral Vectors: Ability to Form Interpolyelectrolyte Complexes and to Mediate Transfection in Vitro. *Biomacromolecules* **2001**, *2* (3), 1023–1028. https://doi.org/10.1021/bm010079f.

(34) Vernon, B.; Tirelli, N.; Bächi, T.; Haldimann, D.; Hubbell, J. A. Water-Borne, in Situ Crosslinked Biomaterials from Phase-Segregated Precursors. *J. Biomed. Mater. Res. Part A* **2003**, *64A* (3), 447–456. https://doi.org/10.1002/JBM.A.10369.

(35) Guerre, M.; Ameduri, B.; Ladmiral, V. One-Pot Synthesis of Poly(Vinylidene Fluoride) Methacrylate Macromonomers via Thia-

Michael Addition. *Polym. Chem.* **2016**, *7* (2), 441–450. https://doi.org/10.1039/c5py01651g.

(36) Ladmiral, V.; Charlot, A.; Semsarilar, M.; Armes, S. P. Synthesis and Characterization of Poly(Amino Acid Methacrylate)-Stabilized Diblock Copolymer Nano-Objects. *Polym. Chem.* **2015**, *6* (10), 1805–1816. https://doi.org/10.1039/C4PY01556H.

(37) Folgado, E.; Mayor, M.; Ladmiral, V.; Semsarilar, M.; Capriati, V.; Yagupolskii, Y.; Mcphee, D. J. Evaluation of Self-Assembly Pathways to Control Crystallization-Driven Self-Assembly of a Semicrystalline P(VDF-Co-HFP)-b-PEG-b-P(VDF-Co-HFP) Triblock Copolymer. *Mol. 2020, Vol. 25, Page 4033* **2020**, *25* (17), 4033. https://doi.org/10.3390/MOLECULES25174033.

(38) Zhang, X.; Xi, W.; Huang, S.; Long, K.; Bowman, C. N. Wavelength-Selective Sequential Polymer Network Formation Controlled with a Two-Color Responsive Initiation System. *Macromolecules* **2017**, *50* (15), 5652–5660. https://doi.org/10.1021/acs.macromol.7b01117.

(39) Kolb, H. C.; Finn, M. G.; Sharpless, K. B. Click Chemistry: Diverse Chemical Function from a Few Good Reactions. *Angew. Chemie Int. Ed.* **2001**, *40* (11), 2004–2021. https://doi.org/10.1002/1521-3773(20010601)40:11<2004::AID-ANIE2004>3.0.CO;2-5.

(40) Anastas, P. T.; Warner, J. C. *Green Chemistry : Theory and Practice*; Oxford University Press: Oxford University Press, New York, 1998.

(41) Li, Z.; Song, G.; He, J.; Du, Y.; Yang, J. Catalyst-Free Sulfa-Michael Addition of Pyrimidine-2-Thiol to Nitroolefins. *J. Sulfur Chem.* **2017**, *38* (6), 686–698. https://doi.org/10.1080/17415993.2017.1369541.

(42) Choudhary, G.; Peddinti, R. K. An Expeditious, Highly Efficient, Catalyst-Free and Solvent-Free Synthesis of Nitroamines and Nitrosulfides by Michael Addition. *Green Chem.* **2011**, *13* (2), 276–282. https://doi.org/10.1039/C0GC00830C.

(43) Vasil'eva, T. P.; Kolomiets, A. F.; Mysov, E. I.; Fokin, A. V. Comparison of α- and β-Trifluoromethylsubstituted Acrylic Acids in Their Reactions with Thiols. *Russ. Chem. Bull.* **1997**, *46* (6), 1181–1183. https://doi.org/10.1007/BF02496227.

(44) Chen, B.; Lei, J.; Zhao, J. Michael Addition of Aryl Thiols to 3-(2,2,2-Trifluoroethylidene)Oxindoles under Catalyst-Free Conditions: The Rapid Synthesis of Sulfur-Containing Oxindole Derivatives. *J. Chem. Res.* **2018**, *42* (4), 210–214. https://doi.org/10.3184/174751918X15240724383170.

(45) Levina, M. A.; Krasheninnikov, V. G.; Zabalov, M. V.; Tiger, R. P. Nonisocyanate Polyurethanes from Amines and Cyclic Carbonates: Kinetics and Mechanism of a Model Reaction. *Polym. Sci. - Ser. B* **2014**, *56* (2), 139–147. https://doi.org/10.1134/S1560090414020092.

(46) Quienne, B.; Poli, R.; Pinaud, J.; Caillol, S. Enhanced Aminolysis of Cyclic Carbonates by β-Hydroxylamines for the Production of Fully Biobased Polyhydroxyurethanes. *Green Chem.* **2021**, *23* (4), 1678–1690. https://doi.org/10.1039/D0GC04120C.

(47) Berne, D.; Cuminet, F.; Lemouzy, S.; Joly-Duhamel, C.; Poli, R.; Caillol, S.; Leclerc, E.; Ladmiral, V. Catalyst-Free Epoxy Vitrimers Based on Transesterification Internally Activated by an α–CF 3 Group. *Macromolecules* **2022**, *55* (5), 1669–1679. https://doi.org/10.1021/acs.macromol.1c02538.

(48) Lemouzy, S.; Cuminet, F.; Berne, D.; Caillol, S.; Ladmiral, V.; Poli, R.; Leclerc, E. Understanding the Reshaping of Fluorinated Polyester Vitrimers by Kinetic and DFT Studies of the Transesterification Reaction. *Chem. – A Eur. J.* **2022**, *28* (48). https://doi.org/10.1002/chem.202201135.

(49) Frisch, M. J.; Trucks, G. W.; Schlegel, H. B.; Scuseria, G. E.; Robb, M. A.; Cheeseman, J. R.; Scalmani, G.; Barone, V.; Mennucci, B.; Petersson, G. A.; Nakatsuji, H.; Caricato, M.; Li, X.; Hratchian, H. P.; Izmaylov, A. F.; Bloino, J.; Zheng, G.; Sonnenberg, J. L.; Hada, M.; Ehara, M.; Toyota, K.; Fukuda, R.; Hasegawa, J.; Ishida, M.; Nakajima, T.; Honda, Y.; Kitao, O.; Nakai, H.; Vreven, T.; Montgomery, J. A.; Peralta, J. E.; Ogliaro, F.; Bearpark, M.; Heyd, J. J.; Brothers, E.; Kudin, K. N.; Staroverov, V. N.; Kobayashi, R.; Normand, J.; Raghavachari, K.; Rendell, A.; Burant, J. C.; Iyengar, S. S.; Tomasi, J.; Cossi, M.; Rega, N.; Millam, J. M.; Klene, M.; Knox, J. E.; Cross, J. B.; Bakken, V.; Adamo, C.; Jaramillo, J.; Gomperts, R.; Stratmann, R. E.; Yazyev, O.; Austin, A. J.; Cammi, R.; Pomelli, C.; Ochterski, J. W.; Martin, R. L.; Morokuma, K.; Zakrzewski, V. G.; Voth, G. A.; Salvador, P.; Dannenberg, J. J.; Dapprich, S.; Daniels, A. D.; Farkas; Foresman, J. B.; Ortiz, J. V; Cioslowski, J.; Fox, D. J. Gaussian 09, Revision B.01. *Gaussian 09, Revision B.01, Gaussian, Inc., Wallingford CT*. 2009.

(50) Grimme, S.; Antony, J.; Ehrlich, S.; Krieg, H. A Consistent and Accurate Ab Initio Parametrization of Density Functional Dispersion Correction (DFT-D) for the 94 Elements H-Pu. *J. Chem. Phys.* **2010**, *132* (15), 154104. https://doi.org/10.1063/1.3382344.

(51) Marenich, A. V.; Cramer, C. J.; Truhlar, D. G. Universal Solvation Model Based on Solute Electron Density and on a Continuum Model of the Solvent Defined by the Bulk Dielectric Constant and Atomic Surface Tensions. *J. Phys. Chem. B* **2009**, *113* (18), 6378–6396. https://doi.org/10.1021/jp810292n.

(52) Bryantsev, V. S.; Diallo, M. S.; Goddard, W. A. Calculation of Solvation Free Energies of Charged Solutes Using Mixed Cluster/Continuum Models. *J. Phys. Chem. B* **2008**, *112* (32), 9709–9719. https://doi.org/10.1021/jp802665d.

Entry for the Table of Contents

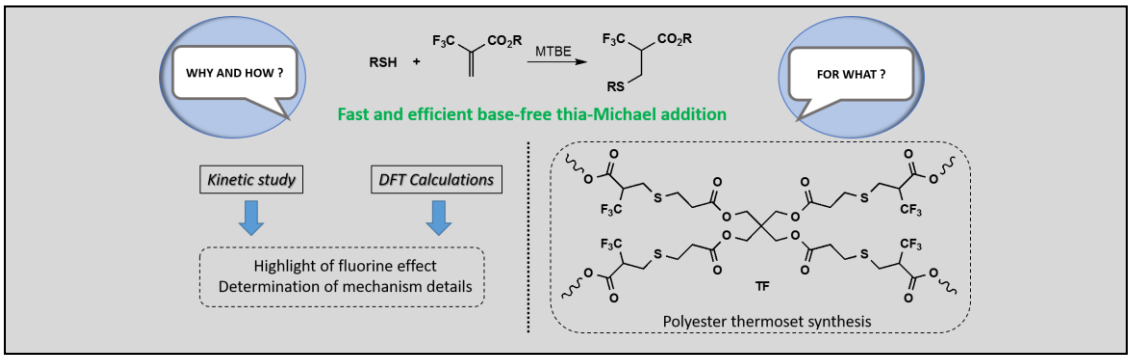

A fast and efficient catalyst-free thia-Michael addition onto α-trifluoromethylacrylates is thoroughly studied through experimental kinetic studies and DFT calculations in order to elucidate its mechanism. An application to a swift preparation of a thermoset is also reported.

Institute and/or researcher Twitter usernames: @chimiebalard, @LCC_CNRS